NMR Determination of the Structures of Peroxycobalt(III) Bleomycin and Cobalt(III) Bleomycin, Products of the Aerobic Oxidation of Cobalt(II) Bleomycin by Dioxygen†

Robert X. Xu,‡ David Nettesheim,‡ James D. Otvos,§ and David H. Petering*,‖

Department of Chemistry, University of Wisconsin-Milwaukee, Milwaukee, Wisconsin 53201, Pharmaceutical Discovery Division, Abbott Laboratories, Abbott Park, Illinois 60064, and Department of Biochemistry, North Carolina State University, Raleigh, North Carolina 27695

Received July 12, 1993; Revised Manuscript Received November 15, 1993®

ABSTRACT: The oxidation of Co(II)bleomycin A_2 by dioxygen leads to two products, HO_2-Co(III)bleomycin A_2 (form I) and Co(III)bleomycin A_2 (form II). ^1H NMR chemical shift assignments for protons of both forms have been made by two-dimensional NMR spectral techniques. The chemical shifts of protons throughout forms I and II differ from each other and from apobleomycin A_2. NOESY spectra reveal a number of intermediate and long-range ^1H–^1H couplings within the metal-binding domain, between the metal-binding domain and the peptide linker, which connects it and the DNA-binding region of the molecule, and, in form I, between the DNA- and metal-binding domains. Molecular dynamics calculations were carried out based on the NOESY results and an adjustable square pyramidyl ligand geometry around Co(III) composed of nitrogen atoms of the primary and secondary amine groups, pyridine (N5), and amide and imidazole (N1) of the hydroxyhistidine residue. In form I, the bithiazole group folds back across the square pyramid forming a compact structure. Although this conformational feature was not observed in form II, the peptide linker between the metal- and DNA-binding domains in both species shows extensive folding based on a large number of intramolecular interactions.

Bleomycin is an intensively studied glycopeptide antibiotic with clinically useful antitumor properties (Figure 1) (Petering *et al.*, 1990).[1] Because of its metal chelation and DNA-binding properties, the structure is commonly divided into metal- (A, P, and H moieties) and DNA-binding (B and R groups) domains linked by a peptide fragment. In model chemical reactions the drug associates with DNA; then, a metal ion in its reduced state, such as Fe^{2+}, binds to the drug and undergoes oxidation–reductions with dioxygen to generate species that cleave the DNA backbone (Chien *et al.*, 1977; Roy *et al.*, 1981; Sausville *et al.*, 1978a,b). The mechanism of aerobic reaction of Fe(II)Blm with DNA has been the subject of continuing interest. It has been shown that a two-electron reduction of O_2 is necessary to generate the reactive species which initiates the degradation of DNA when bound to the polymer (Burger *et al.*, 1985; Kuramochi *et al.*, 1981; and reaction 1).

$$2\text{Fe(II)Blm} + O_2 + H^+ \rightarrow \underset{\text{(activated FeBlm)}}{HO_2\text{-Fe(III)Blm}} + \text{Fe(III)Blm} \quad (1)$$

The precise nature of the activated species is not known except that it has an oxidation state equivalent to peroxyferric bleomycin (Burger *et al.*, 1981).

Recent papers have drawn a strong analogy between the chemistry of oxidation of Co(II)Blm by O_2 and that of Fe(II)Blm (Burger *et al.*, 1981; Xu *et al.*, 1992a,b). In contrast to the reaction involving Fe(II)Blm, the oxidation of Co(II)-Blm produces two stable products, HO_2-Co(III)Blm and Co(III)Blm, called forms I and II, respectively, which are analogous to the products in reaction 1.

Two-dimensional NMR analyses of the structures and solution conformations of apobleomycin A_2, ZnBlm A_2, and OC-FeBlm A_2 (Akkerman *et al.*, 1988a,b, 1990; Haasnoot *et al.*, 1984; Williamson *et al.*, 1990;) have been previously carried out. In each molecule, NOESY spectra revealed through-space interactions between protons of neighboring moieties in the primary structure of the molecule or between groups brought into apposition by metal ion chelation, but not between groups in the two domains which are farther removed from one another. These results were interpreted to mean that except for the metal-binding domain in ZnBlm A_2 and OC-FeBlm A_2, which fold about the metal ion, these structures adopt extended conformations that lack close points of interaction between the metal- and DNA-binding domains.

A study which examined the Co(III) complex of a metal-binding domain fragment of bleomycin concluded that Co(III) coordinates to five nitrogen donor atoms from the drug (Dabrowiak *et al.*, 1981). These included primary and secondary amines, pyrimidine N5 and imidazole N1 ring nitrogens, and the amide nitrogen of the hydroxyhistidine residue which form a square pyramidyl structure (Figure 1).

It has been found that forms I and II Co(III)Blm have differentially shifted ^1H NMR resonances throughout their spectra, indicating that there are differences in the conformations of their metal-binding and DNA-binding domains. In addition, they have significantly different affinities for DNA (Xu *et al.*, 1992b). Both findings suggest that the two domains

† This research was supported by NIH Grant CA-22184 and American Cancer Society Grants CH-466 and DHP-31.

* To whom correspondence should be addressed.
‡ Glaxo Laboratories.
§ North Carolina State University.
‖ University of Wisconsin—Milwaukee.

® Abstract published in *Advance ACS Abstracts,* January 1, 1994.

[1] Abbreviations: A, β-aminoalanine; P, pyrimidinylpropionamide; H, β-hydroxyhistidine; M, α-D-mannose; G, α-L-gulose; V, methylvalerate; T, threonine; B, bithiazole; S, λ-aminopropyldimethylsulfonium; abbreviations in Figure 1a for the component fragments of Blm A_2 the number or subscript following the letter defines an atom shown in the figure; Blm, bleomycin generally referring to the A_2 congener; Co(III)Blm-A_2, mixture of form I and form II CoBlm; COSY, ^1H–^1H correlated spectroscopy; NOESY, nuclear Overhauser enhancement spectroscopy.

0006-2960/94/0433-907$04.50/0

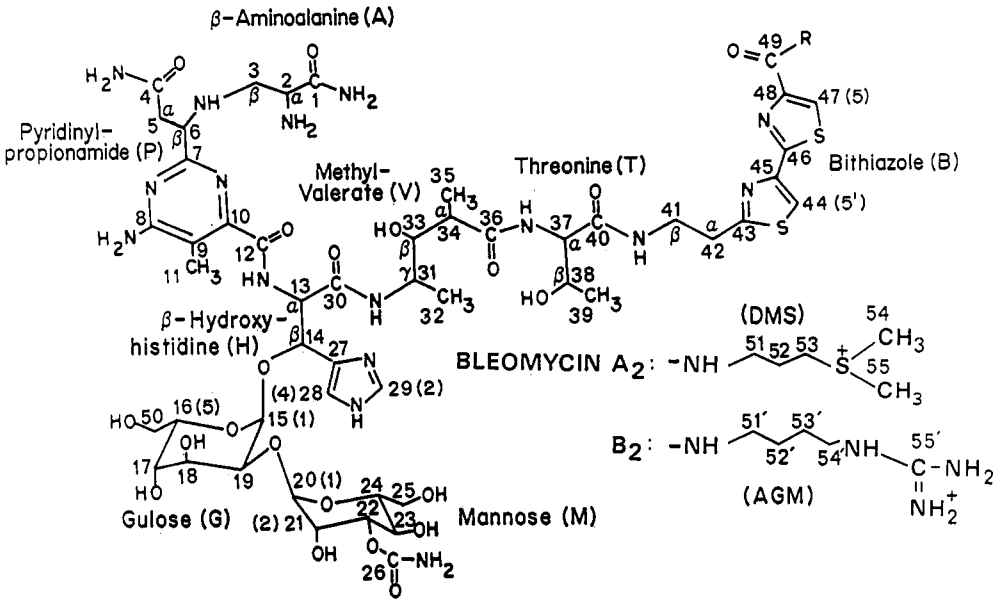

FIGURE 1: Molecular structures of bleomycin A_2 and B_2.

of Co(III)Blm are not isolated from one another as observed in apo-, Zn-, or OC-FeBlm A_2 (Xu *et al.* 1992a,b). To determine the underlying basis for the pervasive differences in chemical shifts of the ^1H resonances of these structures, a detailed NMR study of form I and form II Co(III)Blm has been undertaken.

MATERIALS AND METHODS

Materials. The clinical mixture of bleomycin congeners, comprised mostly of A_2 and B_2 was a gift from Bristol Myers Co. These bleomycins were purified by CM-25 Sephadex column chromatography using a linear gradient of 0.05–0.5 M ammonium formate according to a standard method (Fujii *et al.*, 1973). Form II CoBlm was prepared as described in Xu *et al.* (1992a). Other chemicals were reagent grade.

NMR Spectroscopy. Samples of Blm A_2 or B_2 from CM-Sephadex chromatography were lyophilized, redissolved in water, passed through a Sephadex G-10 column, and relyophilized to remove salt. Equimolar $CoCl_2$ and Blm A_2 or B_2 were mixed in 0.5 mL of 100 mM phosphate–D_2O which maintained pH and prevented freezing of solution at −5 °C. The pH was adjusted to 7.4 with NaOH or HCl. Solutions were then lyophilized. For 2D experiments in H_2O, the dry products were dissolved in 0.5 mL of 90% H_2O/10% D_2O and transferred to a 5-mm NMR tube. When experiments were to be done in D_2O, samples were dissolved in 0.5 mL of 99.8% D_2O and allowed to exchange for 10 min before relyophilization. The resultant material was again dissolved in 0.5 mL of D_2O and transferred to a 5-mm NMR tube for ^1H detection or was dissolved in 2 mL of D_2O and transferred to a 10-mm tube for ^{13}C detection (Akkerman *et al.*, 1988b; Vos *et al.*, 1980). Prior to Fourier transformation, free induction decays (FIDs) of one-dimensional spectra were multiplied by an exponential window function (LB = 0.2 Hz for ^1H; LB = 1 Hz for ^{13}C). For ^1H spectra, the solvent (HDO or H_2O) signal was used as an internal reference (δ = 4.80 ppm at 25 °C or 5.15 ppm at −5 °C). All 2D experiments were carried out either at 25, 5, or −5 °C.

All spectra were recorded on a GE GN500 NMR spectrometer. Phase-sensitive COSY (Aue *et al.*, 1976), DQF-COSY (Rance *et al.*, 1983), and NOESY (Jeener *et al.*, 1979) spectra were recorded both in D_2O and in H_2O with a data matrix of 1024 (t_2) × 256 (t_1) complex pairs. The States method was used to obtain quadrature detection in t_1 (States *et al.*, 1982). The spectral width was 5000 Hz in D_2O and 6410.2 Hz in H_2O in both dimensions. Zero-filling in t_1 was employed to yield a final absorptive spectrum of 1024 × 1024 data points. Since Blm has a short correlation time, the NOE buildup rate is very slow. Thus, the mixing time for the NOESY spectra was 300 ms. In addition, the sample was cooled to −5 °C to increase the correlation time. The carrier frequency was set at the solvent resonance.

For the ^{13}C–^1H HMQC experiment (Bax & Subramanian, 1986), the TPPI method was used to obtain quadrature detection in t_1 (Marion & Wüthrich, 1983). A total of 2K data points were recorded in t_2 with 512 increments in t_1. Aliphatic and aromatic regions were recorded separately.

Structure Calculation. A total of 37 NOE-derived distance restraints for form I conformation and 35 for form II conformation were employed. The restraints were set to 1.8–4.0 Å. For methyl protons, another 1.0 Å was added to the upper bound of the restraints to compensate for center averaging. For methylene protons, 0.6 Å was added to the upper bound of the restraints for the same reason. The NOE force constant was maintained at 50 kcal·mol^{-1}·Å^{-2} throughout the calculations.

A square pyramid geometry of the bleomycin ligands to cobalt was assumed. It was defined by bond angles and a force constant of 100 kcal·mol^{-1}·rad^{-2}. The bond lengths of the nitrogen atoms to cobalt were set with a force constant of 300 kcal·mol^{-1}·Å^{-2} at 2.20 Å for the axial nitrogen, 2.10 Å for the secondary amine, 1.90 Å for pyrimidine nitrogen, and 2.00 Å for the other nitrogens.

The structure calculation was carried out using the software XPLOR/DG (Brünger, 1988; Kuszerski *et al.*, 1992) on a Silicon Graphics 4D-240 computer. One hundred embedded structures were generated from a randomized model structure of cobalt bleomycin with peroxyl (form I) or water (form II) as the sixth ligand. A protocol of restrained molecular dynamics/simulated annealing (SA) (Nilges *et al.*, 1988) was applied to the embedded structures. This protocol consists of three steps.

(Step 1) A Powell energy minimization was performed with van der Waals (VDW) radii to be 0.5 times the CHARMM

values (Brooks *et al.*, 1983) and VDW force constant of 20 kcal·mol^{-1}·Å^{-2}. Then the molecular dynamics calculation was carried out at 2000 K for 7.5 ps, during which the VDW constant decreased from 20 to 0.003 kcal·mol^{-1}·Å^{-2} while the other constants increased from 0.1 to 1.0 times their values or 0.05 to 1.0 times the improper energy.

(Step 2) An annealing procedure was carried out. The temperature dropped from 2000 to 100 K in decrements of 50 K. The VDW radii were decreased from initial 0.9 to final 0.75 of their CHARMM values, while the VDW constant increased from an initial value of 0.003 up to 4.0 kcal·mol^{-1}·Å^{-2}. Each step took 0.25 ps.

(Step 3) One thousand steps of Powell energy minimization were done with the final annealing constants. Finally, a Powell energy minimization with full Lennard-Jones energy of the CHARMM function further refined the structures. The final structures with the lowest total energy were selected, and an average structure from the selected structures was calculated and its energy minimized.

RESULTS

NMR Assignments of CoBlm-A_2. The one-dimensional ^{1}H NMR spectrum of the reaction product(s) of the oxidation of Co(II)Blm-A_2 by molecular oxygen showed immediately that two species were present in equal concentration when it was compared with the spectrum for Blm-A_2 (Xu *et al.*, 1992a). The resonances were assigned to the two species, designated forms I and II, by comparing the one-dimensional ^{1}H spectrum of the mixture with that of form II, which increased at the expense of form I over several months at pH 7 or during a 12-h incubation at pH 1.4 (Xu *et al.*, 1992a). Since form I is relatively unstable in the absence of form II, examination of the NMR properties of form I was done with the mixture of forms I and II.

To assign the resonances of forms I and II to the protons in the bleomycin A_2 structure, the various spin systems of the molecule were matched to the connectivity patterns in COSY and NOESY spectra of forms I and II Co(III)Blm A_2 in D_2O. Using common chemical shift and spin coupling principles, structural assignments for protons of isolated form II were made. Then, by subtraction of these resonances from spectra of the mixture, resonance assignments for form I were established.

Methyl Groups of Pyrimidine and Dimethylsulfonium Moieties. From the peak intensities, shapes, and chemical shifts alone, the methyl group of the substituted pyrimidine and the two methyl groups of the sulfonium moiety could be readily distinguished (Table 1). The assignment of the latter groups was confirmed by comparing the 2D spectra of CoBlm A_2 and CoBlm B_2, which does not contain the dimethylsulfonium group.

Hydroxyhistidine and Bithiazole Aromatic Resonances. In the aromatic region of the 1D spectrum in D_2O, there are only four resonances from each form arising from bithiazole B5 and B5′ and imidazole H2 and H4 protons (Figure 2). The COSY spectrum of the mixture of Co(III)Blm-A_2 structures contained only one cross-peak for each form among these resonances, which distinguished the two histidine proton resonances (which have a weak four bond coupling) from the two isolated bithiazole protons. Since the B5 hydrogen is closer to a carbonyl group and should experience a greater deshielding effect than B5′, the B5 proton was assigned to the lower field bithiazole peak (Table 1).

The H_α and H_β resonances were found at 5.01 and 5.56 ppm for form I and 5.06 and 5.58 ppm for form II at 25 °C (Figure 3). In the NOESY spectrum for CoBlm considered below, one of the pair of H_α and H_β resonances correlated with one of the imidazole resonances in both forms I and II. According to Figure 1 and with a knowledge of bond lengths and angles in the hydroxyhistidine moiety, only H_β and H4 are close enough to exhibit a through-space interaction. Thus, this NOE cross-peak defined H_β and H4 and, secondarily, the assignment of H_α and H2 (Table 1).

Threonine and Valerate Resonances. At high field (0.6–1.3 ppm), there were three peaks for each form which are due to TCH_3, $V_\alpha CH_3$ and $V_\gamma CH_3$ (Figure 1). They were used as the starting point in the identification of threonine (T) and valerate (V) spin systems. The resonances of the T spin network were found at 1.22, 4.27, and 4.40 ppm in form I. Form II has a similar spin pattern and set of resonances (Figure 3). Beginning with the $V_\alpha CH_3$ and $V_\gamma CH_3$ resonances, V_α

Table 1: NMR Chemical Shift Assignments for Protons in Different Bleomycin A_2 Species[a]

peak assignment	apo-Blm	CoBlm form I	CoBlm form I[b]	CoBlm form II	CoBlm form II[b]	Zn-Blm1c	OC-FeBlm[d]
A_α	4.09[e]	3.47	3.38	3.48	3.44	3.75	3.76
A_β	3.10	2.81	2.72	2.90	2.82	2.52	2.42
A_β'	3.10	3.22	3.23	3.29	3.31	3.37	2.88
ANH			6.01		6.92		
P_α	2.65	3.25	3.34	3.28	3.24	2.90	2.93
P_α'	2.75	3.56	3.52	3.54	3.49	3.31	3.18
P_β	4.02	5.18	5.43	5.08	5.07	4.56	4.43
PCH_3	2.05	2.52	2.47	2.55	2.52	2.41	2.33
H_α	5.10	5.01	5.00	5.06	5.08	4.87	5.05
H_β	5.30	5.56	5.52	5.58	5.57	5.21	5.26
H2	7.88	8.71	8.73	8.68	8.64	8.04	7.79
H4	7.32	7.64	7.59	7.67	7.62	7.33	7.26
V_α	2.49	1.03	0.95	1.18	1.09	1.95	2.34
V_β	3.74	3.38	3.37	3.39	3.43	3.38	3.65
V_γ	3.90	3.54	3.51	3.52	3.51	3.63	3.65
$V_\alpha CH_3$	1.14	0.67	0.62	0.75	0.72	0.98	1.03
$V_\gamma CH_3$	1.15	1.00	1.02	0.92	0.92	0.93	1.01
VNH	8.20	8.82	8.92	10.10	10.22		
T_α	4.24	4.40	4.41	4.18	4.11	4.14	4.11
T_β	4.11	4.27	4.27	4.06	4.02	4.03	4.00
TCH_3	1.12	1.22	1.22	1.13	1.12	1.04	1.04
TNH	7.92	8.80	8.97	8.85	9.12		
B_α	3.28	3.12	3.07	3.32	3.27	3.22	3.08
B_α'	3.28	3.32	3.26	3.32	3.27	3.22	3.12
B_β	3.64	3.32	3.45	3.68	3.60	3.59	3.35
B_β'	3.64	3.48	3.86	3.74	3.70	3.59	3.51
B5	8.22	8.24	8.14	8.29	8.21	8.21	8.11
B5′	8.03	7.92	7.81	8.14	8.04	8.04	7.85
BNH			8.62		8.54		
S_α	3.42	3.41	3.42	3.41	3.42	3.36	3.31
S_β	2.20	2.20	2.18	2.20	2.18	2.16	2.09
S_γ	3.62	3.65	3.62	3.65	3.62	3.59	3.53
$S(CH_3)_2$	2.93	2.98	2.99	2.95	2.94	2.90	2.83
SNH			9.04		9.04		
G1	5.30	5.38	5.38	5.37	5.38	5.31	5.28
G2	4.08	4.15	4.13	4.15	4.13	4.09	4.08
G3	4.12	4.13	4.12	4.13	4.12	4.06	4.08
G4	3.87	3.82	3.83	3.82	3.83	3.73	3.78
G5	4.02	3.83	3.83	3.83	3.83	3.87	3.82
G6	3.46	3.73	3.76	3.73	3.76	3.64	3.66
G6′	3.58	3.76		3.76		3.73	3.76
M1	5.03	4.96	4.94	4.96	4.94	4.91	4.95
M2	4.09	3.99	4.02	3.99	4.02	4.09	4.11
M3	4.70	3.98	4.00	3.98	4.00	4.08	4.21
M4	3.81	3.86	3.88	3.86	3.88	3.72	3.70
M5	3.81	3.87	3.89	3.87	3.89	3.72	3.74
M6	3.81	3.87	3.71	3.73	3.71	3.82	3.81
M6′	3.92	3.76		3.76		3.98	3.91

[a] Apo-Blm and CoBlm I and II were in phosphate buffer, pH 7.4, at 25 °C except as noted; ZnBlm was at pH 7.6 and 27 °C in the absence of buffer; OC-FeBlm was at pH 7 and 25 °C in the absence of buffer. [b] Temperature was −5 °C. [c] Akkerman *et al.* (1988a). [d] Akkerman *et al.* (1990). [e] ppm.

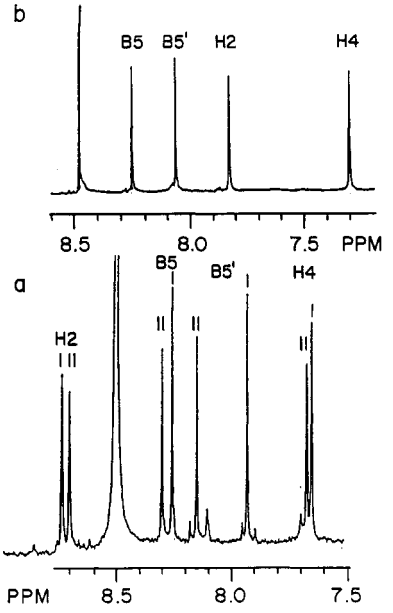

FIGURE 2: One-dimensional ^1H NMR spectra of the oxidation product(s) of the reaction of Co(II)Blm A_2 with O_2 (a) and Blm A_2 (b). Aromatic region [taken from Xu *et al.* (1992b) with permission].

and V_γ were defined by COSY cross-peaks at 1.03 and 3.54 ppm in form I and 1.18 and 3.52 ppm in form II (Figure 3). COSY spectra of Co(III)Blm A_2 in H_2O showed that two downfield resonances also display a cross-peak with an amide proton at 8.82 ppm for form I and 10.10 ppm for form II. Therefore, the resonances at 3.52 and 3.54 ppm were identified as V_γ and the others as V_α protons.

The V_β proton had only weak COSY correlations with V_α and V_γ; the cross-peaks could only be seen on a very low contour plot. Nevertheless, the position of V_β was confirmed by NOESY spectra, in which V_β had strong cross-peaks with V_α, $V_\gamma CH_3$, and $V_\alpha CH_3$ in each form.

R Group Protons. The $-CH_2-CH_2-CH_2-$ group in the tail of CoBlm A_2 was distinguished easily by two strong COSY cross-peaks in Figure 3, which correlated S_β (2.20 ppm) with S_α (3.41 ppm) and S_γ (3.48 ppm). With the additional definition of a cross-peak between S_α and an adjacent amide proton at 9.04 ppm when COSY spectra were taken in H_2O, the assignment of the three resonances to specific protons was complete.

β-Aminoalanine and Pyrimidinyl Propionamide Group. Two spin systems, A (A_α, A_β, A_β') and P (P_β, P_α, P_α'), were located in the COSY spectrum of the CoBlm mixture (Figure 3). The secondary amine protons of β-aminoalanine, ANH, were at a distance of three bonds from the CH_2 hydrogen of this moiety (A_β and A_β') and three bonds from CH of propionamide (P_β). In NOESY spectra of samples dissolved in H_2O, a secondary amine resonance was found having two cross-peaks identified as A_β and A_β' for each form (Supplementary Material). Accordingly, the A and P systems were defined (Table 1).

Bithiazole Aliphatic Protons. The COSY spectrum of CoBlm A_2 in D_2O in Figure 4defined this system. Additional information from the COSY spectrum pattern in water at −5

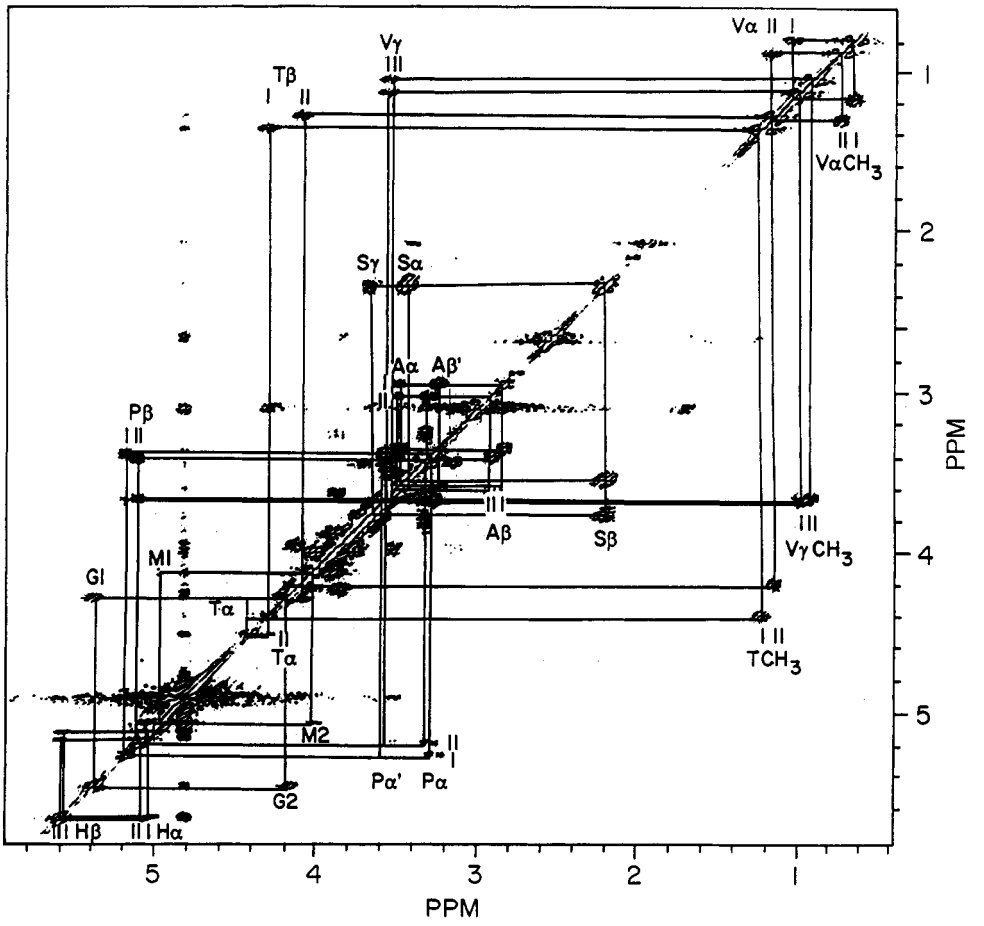

FIGURE 3: Contour plot of the 3–6 ppm region of the phase-sensitive COSY of CoBlm A_2 in D_2O, 1.0 mM CoBlm A_2, and 10 mM phosphate, pH 7.4, 25 °C. The assignments of cross-peaks correspond to their horizontal chemical shifts. Forma I and II are indicated as I and II, respectively, in this and successive figures.

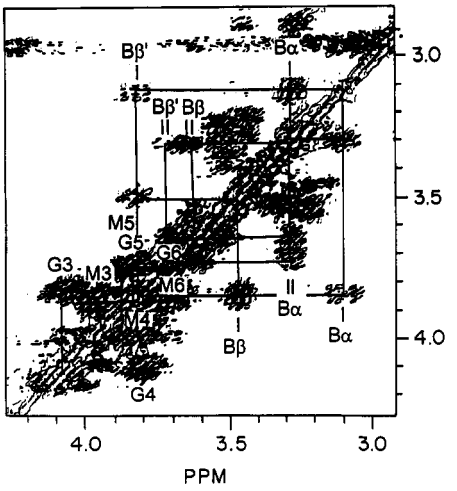

FIGURE 4: Contour plot of the 2.9–4.5 ppm region of the phase-sensitive COSY of CoBlm A_2 in D_2O, 1.0 mM CoBlm A_2, and 10 mM phosphate, pH 7.4, 25 °C.

°C indicated that an amide peak formed a cross-peak with B_β and B_β' of each form, thus differentiating B_β from B_α.

Disaccharide Protons. The two sugar rings, gulose and mannose, have 12 proton resonances crowded into the 3.7–4.2 ppm region of the 1D spectrum. Because of their unique environment, G1 and M1 are located further downfield. As seen in Figure 3, G1 and M1 protons made cross-peaks with those identified with G2 and M2. Calculations suggest that if G1 and M1 are in equatorial position, G1–G2 should display a larger coupling constant (3.6 Hz) than M1–M2 (1.8 Hz) (Bax & Subramanian, 1986). Thus, the stronger cross-peak was thought to correlate G1 and G2. NOE cross-peaks linking G1 with H_β and H4 were also consistent with this assignment.

It was difficult to find other cross-peaks which could continue the linkage process from G2 and M2 to G3 and M3, respectively. However, ^1H–^{13}C COSY spectra showed that there are two other resonances near the G2 and M2 proton chemical shifts. If these resonances are G3 (4.13 ppm) and M3 (3.98 ppm), their cross-peaks with G2 (4.15 ppm) and M2 (3.99 ppm) may be too close to the diagonal to be observed. On the basis of this reasoning, the G3 and M3 proton were assigned. Other cross-peaks related to G3 and G4 (3.82 ppm) and M3 and M4 (3.86 ppm) (Figure 4). Again, ^1H–^{13}C COSY spectra helped to locate and identify G5 (3.83 ppm) and M5 (3.87 ppm). From there, G6, G6′ and M6, M6′ resonances were tentatively assigned near 3.73 and 3.76 ppm (Figure 4).

Except for G1, the 2D spectra of the disaccharide from freshly prepared samples, which contained equal amounts of forms I and II, were similar to older samples composed mainly of form II. This fact indicated that the sugar moieties of Blm are not differentially affected in the two Co(III) species.

NOESY Spectra of the Two Forms of CoBlm A_2. According to Table 1 the chemical shifts of protons throughout the structures of forms I and II differ from one another. Differences of greater than 0.1 ppm are common even in regions of the structures not expected to be part of the metal-binding site (Itaka *et al.*, 1978; Derome, 1987; Chien *et al.* 1977). In addition, in apo-Blm A_2, the bithiazole α- and β-CH_2 protons exhibit only one chemical shift for each methylene group (Table 1). In contrast, the β-CH_2 group nearer to BNH in form II Co(III)Blm A_2 has two different chemical shifts, indicating that this carbon is rotationally constrained leading to the inequivalence of its two protons. In contrast, the α-CH_2 carbon still displays degenerate ^1H chemical shifts. Finally, both α- and β-CH_2 groups in form I display pairs of inequivalent

Table 2: Nonvicinal NOE Couplings on Forms I and II CoBlm A_2

		form I[a]	
A_α – H2	H_β – G1	VNH – $V_\gamma CH_3$	TNH – TCH_3
A_β – ANH	H_β – G2	VNH – V_β	TNH – T_β
$A_{\beta'}$ – H2	H_β – V_α	V_α – TNH	T_α – BNH
$A_{\beta'}$ – ANH	H_β – H4		T_α – TCH_3
ANH – H2	H2 – V_α	$V_\alpha CH_3$ – Vγ	T_β – BNH
	H2 – $V_\alpha CH_3$	$V_\alpha CH_3$ – TNH	TCH_3 – BNH
PCH_3 – B5	H2 – TCH_3	V_β – TNH	
	H4 – $V_\alpha CH_3$	V_β – $V_\alpha CH_3$	
	H4 – V_α	V_β – $V_\gamma CH_3$	
		V_β – B5′	
		$V_\gamma CH_3$ – B5′	

[a] Form II has same NOEs except for the following: it has BNH-B_α and lacks B5-PCH_3 and B5′-V_β.

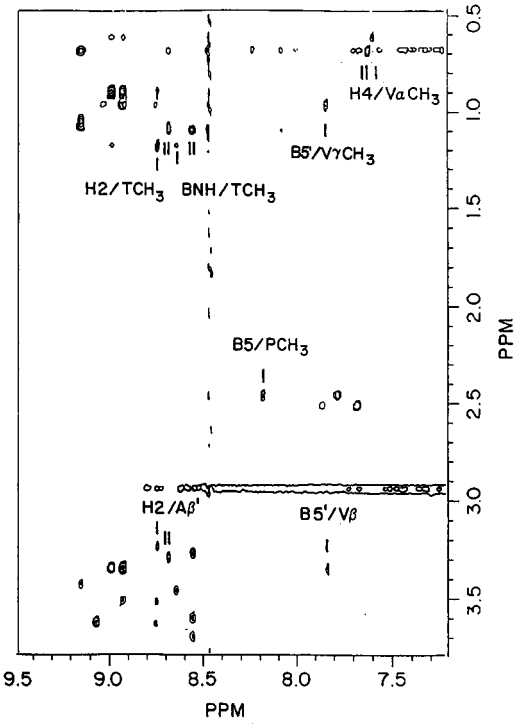

FIGURE 5: Contour plot of the 6.7–9.6 ppm versus 0.5–3.8 ppm region of the NOESY of CoBlm A_2 in H_2O, 6.0 mM CoBlm A_2, and 30 mM phosphate, pH 7.4, –5 °C.

hydrogens. This progressive decrease in conformational degrees of freedom confirms the differences in solution conformation of parts of apo-Blm A_2, form II, and form I near the DNA binding domain of the drug. Thus, it is likely that forms I and II adopt different overall conformations, which are each distinguishable from apo-Blm in the non-metal-binding portion of the molecule.

To examine detailed conformational features of forms I and II, NOESY spectra were acquired at –5 °C. A number of medium and long-range NOEs were observed in one or both forms in addition to shorter range interactions between non-vicinal hydrogens (Table 2). Figures 5 and 6 point out key longer range interactions. Several NOEs were found between H2 and protons of A (A_α, A_β', ANH) and between H4 and H_β, which indicate that potential metal-binding ligands of the imidazole, primary, secondary amine, and hydroxyhistidine amide groups are drawn together in forms I and II as a result of metal ion complexation. H2, H4, and H_β protons are also close to hydrogens of the V (H2-V_α, H2-$V_\alpha CH_3$, H4-$V_\alpha CH_3$, H4-V_α, H_β-V_α) and T (H2-TCH_3, H2-TNH) residues. Apparently, metal complexation establishes conformational constraints between the metal-binding domain and the peptide region that links the metal- and DNA-binding

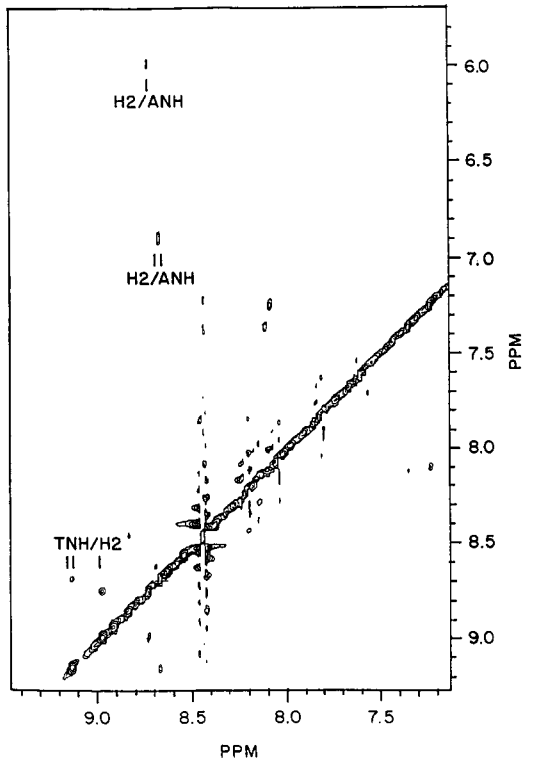

FIGURE 6: Contour plot of the 7.2–9.4 ppm versus 5.7–9.2 ppm region of the NOESY of CoBlm A_2 in H_2O, 6.0 mM CoBlm A_2, and 30 mM phosphate, pH 7.4, –5 °C.

domains of the structure. Protons of the bithiazole moiety also exhibit a number of long-range NOE interactions (B5′-$V_\gamma CH_3$, BNH-TCH_3, and B5-PCH_3 and B5′-V_β for form I). According to these results, the DNA-binding domain also is in conformational proximity to the linker region and, in form I, to the metal-binding domain as well.

Molecular Dynamics Calculations of the Conformations of Forms I and II. Structure calculations for both forms I and II were carried out according to the process described under Materials and Methods. The 24 lowest energy structures of form I divide themselves among two overall structures A and B (Figure 7a,b; Table 3). In both, the DNA-binding region of the molecule is folded back upon the Co-binding domain. A basic difference between them is that the metal centers of A and B have opposite chiralities. That is, the Co-binding ligands wrap themselves around the metal ion in two ways. This leads to two different folded conformations in which the bithiazole moiety lies on different sides of the equatorial plane of the metal-binding sites and in proximity to either the axial peroxide (configuration A) or primary amine (configuration B). Apart from this difference and differing conformations for the disaccharide moieties, the rest of the two structures display clearly similar folding from the bithiazole group through the metal-binding domain. Both forms exist as close-packed structures in which virtually all the atoms except those in the positively charged tail and the disaccharide make multiple van der Waals contacts with other parts of the molecule.

The lowest energy structures of form II also display two chiralities for the cobalt center with B predominating over A, 11 to 5. An average structure was not generated because the bithiazole group was not restricted to a definite conformation in any of the individual form II structures. Thus, as an example of such structures, the lowest energy form is shown in Figure 7c. Although the bithiazole does not interact with the metal-binding domain, the rest of the peptide linker region is folded and in van der Waals contact with the metal-binding region.

A molecular dynamics simulation was also carried out on form II without inclusion of NOE restrictions. As expected, the average total energy among the 21 lowest energy structures was higher (8.7 kcal/mol) than among conformations obtained with the guidance of NOESY conformation (Table 3). There was no chiral preference for the metal center (11 and 10 structures with A and B configurations, respectively). In all cases there was folding within the linker region; 16 adopted a form II-like conformation, three folded like form I in the A configuration, and two could not be classified as related to either form.

DISCUSSION

In the oxidation of Co(II)Blm by dioxygen, two different diamagnetic Co(III) structures are formed (reaction 2) as indicated by the presence of two independent sets of ^1H NMR resonances in the product mixture (Table 1; Xu *et al.*, 1992a).

$$2\text{Co(II)Blm} + O_2 + H^+ \rightarrow \underset{\text{form I}}{HO_2\text{-CO(III)Blm}} + \underset{\text{form II}}{\text{Co(III)Blm}} \quad (2)$$

This is also shown in the isolation of two species by HPLC, which are then identifiable by NMR analysis with the two products in the redox reaction (Xu *et al.*, 1992a). One of these compounds, called form I, has peroxide bound to it; the other, form II, does not (Xu *et al.*, 1992a). According to mechanistic studies, they are produced in a dimerization reaction that also appears to occur in the presence of DNA (reactions 3 and 4) (Xu *et al.*, 1992a,b):

$$2O_2\text{-CoBlm} \rightarrow \text{BlmCo-}O_2\text{-CoBlm} + O_2 \quad (3)$$

$$\text{BlmCo-}O_2\text{-CoBlm} + H^+ \rightarrow HO_2\text{-Co(III)Blm} + \text{Co(III)Blm} \quad (4)$$

In the present study all of the ^1H NMR resonances of forms I and II have been assigned primarily by COSY analysis with the exception of the resonances in the disaccharide unit. It is evident from Table 1 that small differences in chemical shift of resonances exist throughout forms I and II. Relative to Blm A_2 both species display changes in chemical shift of ≥0.1 ppm in every resonance of moieties A, P, H, and V and several resonances of G and M (Figure 1). In form I all of the chemical shifts of protons in T are perturbed significantly from apo-Blm as are most of those in B. Some resonances in T and B also are perturbed in form II. Only the protons of the dimethylsulfonium tail experience little change in chemical shift. These changes in chemical shifts are more pervasive than those reported for ZnBlm A_2, in which the chemical environments of protons in T and B hardly change in comparison with those of Blm A_2, but they resemble the widespread changes in ^1H resonance positions in OC-FeBlm A_2 (Table 1). Thus, the discrete segregation of the structure of the drug into noninteracting metal- and DNA-binding domains on the basis of NMR chemical shift analysis, which works for ZnBlm A_2 and has also been suggested for OC-FeBlm, is not an adequate model for either form I or II CoBlm and probably not for OC-FeBlm (Akkerman *et al.*, 1988a,b, 1990).

Previous definition of the structure and conformation of the coordination sphere of various metallobleomycins has been based on X-ray crystallographic or NMR analysis. Idealized configurations of the metal-binding sites for each are shown

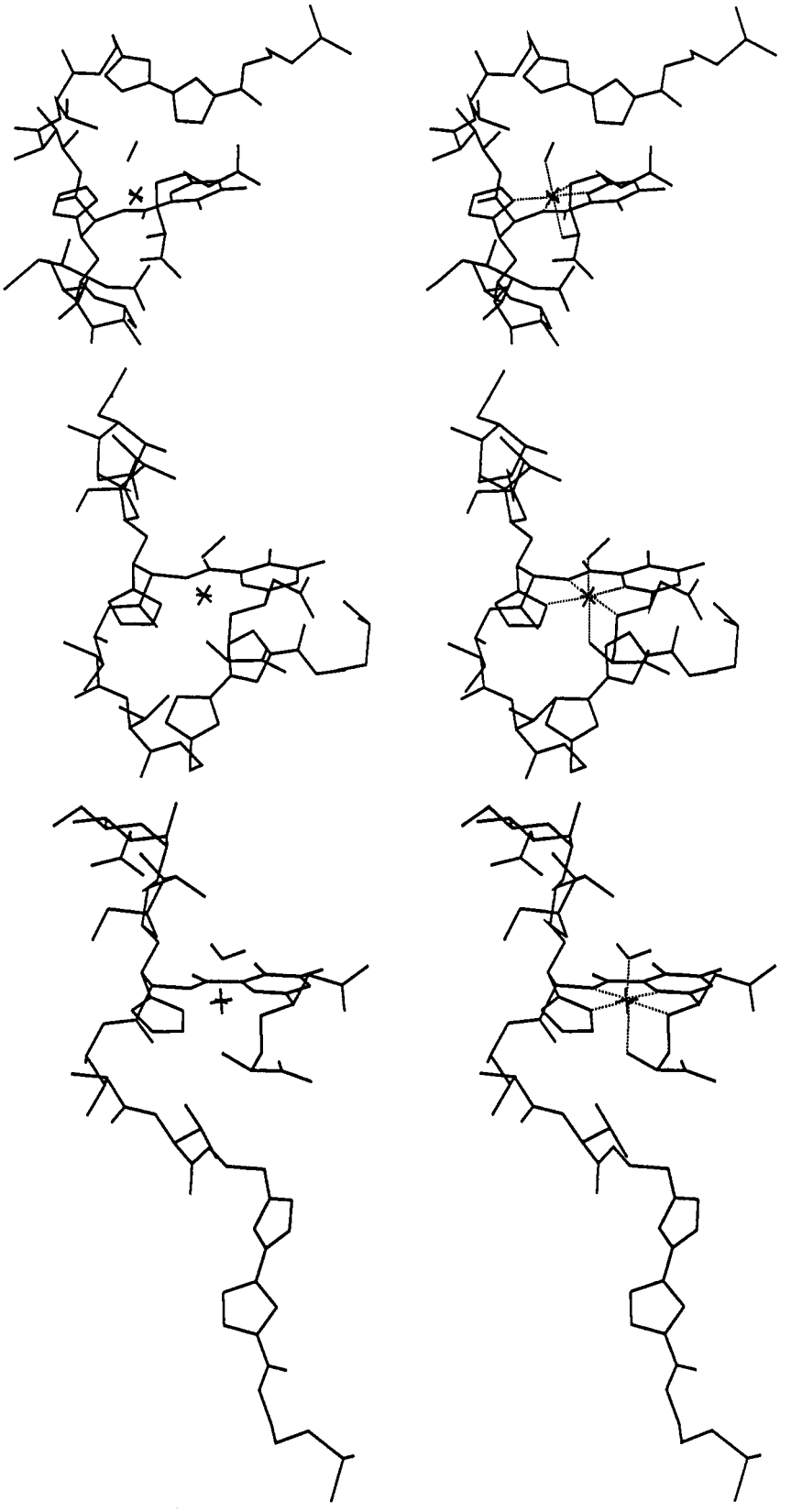

FIGURE 7: Conformations of forms I and II Co(III)Blm A_2 based on molecular dynamics calculations. Energy-minimized average conformations for (a, top) form I (metal-binding domain configuration A) and (b, middle) form I (configuration B). (c, bottom) Lowest energy conformation of form II with the sixth ligand as water (configuration B).

in Figure 8. The same five nitrogen ligands comprise the coordination sphere in CuP-3a and the low-temperature forms of CoBlm-primary and secondary amine nitrogen atoms from A, pyrimidine N5 from P, and amide and imidazole N1 nitrogens from H (Iitaka *et al.*, 1978). In ZnBlm, the carbamoyl nitrogen of mannose adds to this array in a sixth position (Akkerman *et al.*, 1988a). According to an NMR study of OC-FeBlm, the carbamoyl nitrogen replaces the primary amine group bound in ZnBlm and CO is ligated to the sixth binding site (Akkerman *et al.*, 1990). The firm ligation of a carbamoyl nitrogen to Zn or Fe is doubtful because of its poor metal-binding characteristics, particularly if it must

Table 3: Structural Statistics for 24 Peroxycobalt(III) Bleomycin Structures

	conformation A[a]		conformation B[a]	
	SA_i	AV_m	SA_i	AV_m
rmsd from distance restraints (Å)	0.0045 ± 0.0054	0.0040	0.00067 ± 0.0084	0.000
rmsd from idealized geometry				
bond (Å)	0.0088 ± 0.0001	0.0090	0.0087 ± 0.0003	0.0085
angles (deg)	1.63 ± 0.01	1.63	1.65 ± 0.01	1.65
impropers (deg)	0.33 ± 0.01	0.33	0.33 ± 0.02	0.31
conformational energy (kcal/mol)[b]				
E^{total}	−2.66 ± 4.63	−4.98	−5.25 ± 2.68	−5.42
E_{NOE}[c]	0.088 ± 0.157	0.029	0.208 ± 0.286	0.000
E_{L-J}[d]	−45.5 ± 4.1	−48.6	−47.5 ± 2.2	−46.9
E_{bond}	5.54 ± 0.22	5.81	5.26 ± 0.35	5.07
E_{angle}	35.9 ± 1.6	36.5	35.5 ± 2.1	35.3
$E_{improper}$	1.27 ± 0.09	1.29	1.27 ± 0.16	1.11
atomic rmsd for all heavy atoms				
SA_i vs AV^a	1.84 ± 0.46		1.81 ± 0.64	

[a] SA_i is the ensemble of the 16 final structures with conformation A or eight final structures with conformation B, AV is the mean atomic structure of A or B conformations, and AV_m is the energy-minimized mean atomic structure of A or B conformations. [b] All energies are in kcal/mol. [c] E_{NOE} is the energy contribution from the square-well NOE potential with a force constant of 50 kcal·mol^{-1}·Å^{-2}. [d] E_{L-J} is the Lennard-Jones van der Waals energy calculated using the CHARMM function (Brooks *et al.*, 1988).

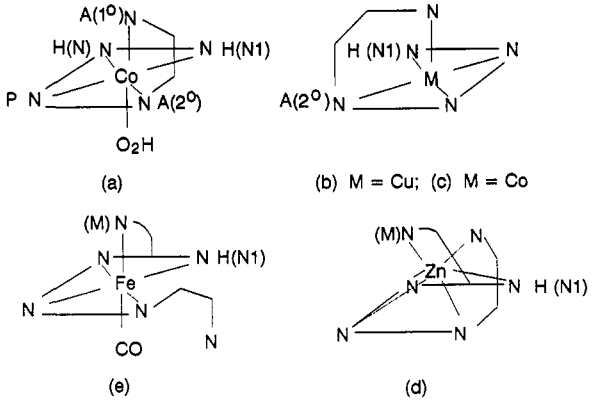

FIGURE 8: Chirality of metal-binding domain of metallobleomycin structure. Amine alaninamide (A) primary (1°) and secondary (2°); pyrimidine (P) N5 nitrogen; histidine amide (HN), and histidine imidazole (H) N1 nitrogen; mannose (M) carbamoylnitrogen. (a) Form I CoBlm; (b) CuP-3A (Iitaka *et al.*, 1978); (c) Co(III)-pseudotetrapeptide A of Blm (Dabrowiak & Tsukayama, 1981); (d) ZnBlm (Akkerman *et al.*, 1988a); and (e) OC-FeBlm (Akkerman *et al.*, 1990).

replace a primary amine group opposite carbon monoxide in OC-FeBlm.

Examination of medium and long-range NOEs of forms I and II with the XPLOR/DG molecular dynamics program has made possible the definition of the overall three-dimensional conformations of these molecules (Figure 7). It was shown that the peptide linker folds into definite conformations in forms I and II and that, in form I, the bithiazole group is folded back upon the cobalt-binding domain.

The XPLOR/DG program considers both chiral configurations of ligands about the Co(III) center in the molecular dynamics calculation. According to the results there is a strong though not exclusive preference for configuration A among the lowest energy conformations of form I and, likewise, a strong preference for the other configuration B in form II (Figure 7). Reversal of the axial amine and peroxide groups in either configuration converts it into the other one. Various portrayals of metallobleomycin structures in the literature show either of the two chiralities about various metal ions (Figure 8). However, no mention has been made previously of this feature of the metal-coordination site.

The two configurations A and B for the Co-center, which are derived in the molecular dynamics calculation, surely do not represent solution structures in rapid equilibrium with one another. The two forms could only be interconverted after Co–ligand bond dissociation; this occurs very slowly in Co(III) complexes (Basolo & Pearson, 1972). Instead, they are closely related, calculated structures based on the available NOESY data. The actual distribution of form I among A and B will require further study. Nevertheless, the results of the calculation strongly favor the A configuration.

The chirality of the metal-binding domain is directly related to the overall conformation of the structure. In configuration A (Figure 7a) the linker peptide can only fold back upon itself to bring the bithiazole unit into proximity with the pyrimidyl residue on the same side of the plane of Co-coordination as the axial peroxide group. Attempts to carry out the folding process on the other side lead to prohibitive steric barriers. Conversely, in configuration B only when the bithiazole interacts with the pyrimidine group from the same side as the axial amine can a stable structure be found (Figure 7b).

Form II displays a number of the same NOE interactions between the metal-binding domain and the peptide linker region as detected in form I and, thus, is thought to adopt the same general conformation within this larger fragment of the molecule (Figure 7c). Other NMR evidence supports the differences in overall conformation for forms I and II inferred from the NOESY experiments. In the two forms, H2 and H4 have similar chemical shifts, while the B5′ protons do not, indicative of different chemical environments for the bithiazole moiety in the two structures. Following integration of the aromatic peak areas of forms I and II of several CoBlm samples, it was found that the peak area ratios (I/II) for B5′ were always larger than those for imidazole H2 and H4. For example, in a typical spectrum the ratio for H4 (form I/form II) was 0.33, that for H2 was 0.39, and that for B5′ was 0.47. Because these spectra were obtained under partially relaxed conditions (pulse repetition rate $<4t_1$), it can be inferred that the relative t_1 values for the B5′ protons in the two forms are different from those arising from the imidazole protons. This finding is consistent with the conformational difference between the two forms being localized primarily in the DNA-binding domain.

Previous studies of the conformations of Zn- and OC-FeBlm A_2 assumed that once the metal-binding domain folded about the metal ion, the rest of these structures had extended conformations (Akkerman *et al.*, 1988a, 1990). Nevertheless, in ZnBlm A_2 at 4 °C there is one significant long-range NOE between H4 and $V_\alpha CH_3$ that signifies folding within the linker

peptides relative to the metal-binding site (Akkerman *et al.*, 1988a). In OC-FeBlm there is extensive perturbation of ^{1}H chemical shifts relative to apo-Blm A_2. Futhermore, the large set of NOEs among protons of the interdomain peptide linker is indicative of the presence of a specific conformation within this region (Table 1) (Akkerman *et al.*, 1990). This network is tied to the metal-binding domain by an H_β-VNH interaction. So, in this molecule as in forms I and II CoBlm, the overall structure does not appear to adopt a simple extended conformation.

Form I, HO_2-CoBlm, is considered to be analogous to the activated form of FeBlm, though the detailed structure of that species is not known (Burger *et al.*, 1985). If they do assume the same folded conformation, it would explain the recent finding that the self-degradation of activated Fe(III)-Blm involves, in part, damage to the bithiazole moiety (Nakamura & Peisach, 1988). In the folded structure of form I, the bithiazole makes intimate contact with the peroxide adduct. In such a structure involving activated FeBlm, the bithiazole would be an obvious site for oxidative reaction.

These results and interpretations can be extended to the interaction of CoBlm with DNA. It has been recognized that form I Co(III)Blm A_2 binds more strongly to DNA than does form II (Xu *et al.*, 1992b). The definition of two distinctly different structures for these species in the present study is consistent with this difference in binding affinity. Assuming that form I retains its conformation when bound to DNA, then both nucleotide and metal-binding domains must be in close contact with the DNA polymer. This conclusion was also reached about binding of the dioxygen adduct of Co(II)Blm to DNA (Chikira *et al.*, 1990).

Several other studies have also implied that the metal-binding domain of metallobleomycins interacts with DNA. These include the finding that the ESR spectrum of NO-Fe(II)Blm is perturbed in the presence of DNA, that the CD spectrum of the azide adduct of Fe(III)Blm is altered by DNA, and that the metal-binding domains of Cu(II)- and Fe(III)-Blm are rotationally constrained when bound to DNA (Antholine & Petering, 1979; Albertini & Garnier-Suillerot, 1984; Chikira *et al.*, 1991).

A particularly informative study examined the ^{1}H NMR spectrum of diamagnetic OC-Fe(II)Blm in the absence and presence of poly(dA-dT)·poly(dA-dT) (Brown *et al.*, 1981). In comparison with apo-Blm, in which the bithiazole protons broaden in the presence of DNA, both bithiazole and imidazole protons broaden when OC-Fe(II)Blm binds to DNA. In addition, the imidazole H2 and H4 protons as well as the pyrimidine methyl protons shift position when the complex interacts with the polymer. Evidently, the metal-binding domain of OC-Fe(II)Blm detects the presence of the DNA. Together, the experiments and studies cited here indicate that the metal- and DNA-binding domains of several metallobleomycin species associate with DNA in the drug–polymer binding reaction.

Finally, the possibility that two chiral forms of the metal centers exist in Co(II) or Co(III)Blm and by inference in the corresponding forms of FeBlm has implications for the redox reactions of these complexes when bound to DNA. It has been recognized that for reaction 4 to occur when O_2-CoBlm is bound to DNA, either the adduct had to bind to DNA in two different conformations to bring two O_2-Co groups face to face to dimerize or configurational rearrangement of the axial amine had to occur during the reaction (Xu *et al.*, 1992b). Examining the structure of the metal–ligand site indicates that the latter is an unlikely possibility. Thus, if the metal center is also chiral, four different conformations between DNA and the drug might exist.

ACKNOWLEDGMENT

We thank Dr. Robert P. Meadows and Dr. Andrew M. Petros for very helpful discussions on structure calculations. We also thank Dr. Steven W. Fesik for kindly providing the computing facilities at Abbott Labs.

SUPPLEMENTARY MATERIAL AVAILABLE

Seven figures showing ^{1}H NMR spectra used in assignments of ^{1}H resonances to the form I and II CoBlm A_2 structures and two tables listing NOE couplings in various metallobleomycins (14 pages). Ordering information is given on any current masthead page.

REFERENCES

Akkerman, M. A. J., Haasnoot, C. A. G., & Hilbers, C. W. (1988a) *Eur. J. Biochem. 173*, 211–225.

Akkerman, M. A. J., Haasnoot, C. A. G., Pandit, U. K., & Hilbers, C. W. (1988b) *Magn. Reson. Chem. 26*, 793–802.

Akkerman, M. A. J., Neijman, W. J. F., Wijmenga, S. S., Hilbers, C. W., & Vermel, W. (1990) *J. Am. Chem. Soc. 112*, 7462–7474.

Albertini, J. T., & Garner-Suillerot, A. (1984) *Biochemistry 23*, 47–53.

Antholine, W. E., & Petering, D. H. (1979) *Biochem. Biophys. Res. Commun. 9*, 528–533.

Aue, W. P., Bartholdi, E., & Ernst, R. R. (1976) *J. Chem. Phys. 64*, 2229–2246.

Basolo, F., & Pearson, R. G. (1967) *Mechanisms of Inorganic Reactions*, Chapter 3, John Wiley and Sons, Inc., New York.

Bax, A., & Subramanian, S. (1986) *J. Magn. Reson. 67*, 565–569.

Brooks, B. R., Bruccoleri, R. W., Olafson, B. D., States, D. J., Swaminathan, S., & Karplus, M. J. (1983) *Comput. Chem. 4*, 187–193.

Brown, C., Antholine, W. E., & Petering, D. H. (1981) *Proc. Natl. Acad. Sci. U.S.A. 78*, 7517–7520.

Brünger, A. T. (1988) *XPLOR Manual*, Yale University, New Haven, CT.

Burger, R. M., Peisach, J., & Horwitz, S. B. (1981) *J. Biol. Chem. 256*, 11636–11644.

Burger, R. M., Horwitz, S. B., & Peisach, J. (1985) *Biochemistry 24*, 3623–3629.

Chien, M., Grollman, A. P., & Horwitz, S. B. (1977) *Biochemistry 16*, 3641–3647.

Chikira, M., Antholine, W. E., & Petering, D. H. (1990) *J. Biol. Chem. 264*, 21478–21480.

Chikira, M., Sato, T., Antholine, W. E., & Petering, D. H. (1991) *J. Biol. Chem. 266*, 2859–2863.

Dabrowiak, J. C., & Tsukayama, M. (1981) *J. Am. Chem. Soc. 103*, 7543–7550.

Ehrenfeld, G. M., Shipley, J. B., Heimbrook, D. C., Sugiyama, H., Long, E. C., van Boom, J. H., van der Marel, G. S., Oppenheimer, N. J., & Hecht, S. M. (1987) *Biochemistry 26*, 931–942.

Fujii, A., Takita, T., Maeda, K., & Umezawa, H. (1973) *J. Antibiot. 26*, 396–397.

Haasnoot, C. A. G., Pandit, U. K., Kruk, C., & Hilbers, C. W. (1984) *J. Biomol. Struct. Dyn. 2*, 449–467.

Iitaka, Y., Nakamura, H., Nakatani, T., Muraoka, Y., Fujii, A., Takita, T., & Umezawa, H. (1978) *J. Antibiot. 31*, 1070–1072.

Jeener, J., Meie, B. H., Wingfield, P. T., & Ernst, R. R. (1979) *J. Chem. Phys. 71*, 4546–4553.

Kuramochi, H., Takahashi, K., Takita, T., & Umezawa H. (1981) *J. Antibiot. 34*, 576–582.
Marion, D., & Wüthrich, K. (1983) *Biochem. Biophys. Res. Commun. 113*, 967–974.
Nakamura, M., & Peisach, J. (1988) *J. Antibiot. 41*, 638–647.
Nilges, M., Clore, G. M., & Gronenborn, A. M. (1988) *FEBS Lett. 299*, 317.
Petering, D. H., Byrnes, R. W., & Antholine, W. E. (1990) *Chem.-Biol. Interact. 73*, 133–182.
Rance, M., Sørensen, O. W., Bodenhausen, G., Wagner, G., Ernst, R. R., & Wüthrich, K. (1983) *Biochem. Biophys. Res. Commun. 117*, 479–485.
Roy, S. N., Orr, G. A., Brewer, D. F., & Horwitz, S. B. (1981) *Cancer Res. 41*, 4471–4477.
Sausville, E. A., Peisach, J., & Horwitz, S. B. (1978a) *Biochemistry 17*, 2740–2745.
Sausville, E. A., Stein, R. W., Peisach, J., & Horwitz, S. B. (1978b) *Biochemistry 17*, 2746–2754.
States, D. J., Haberkorn, R. A., & Rueben, D. J. (1982) *J. Magn. Reson. 48*, 286–292.
Vos, C. M., Westera, G., & Schipper, D. (1980) *J. Inorg. Biochem. 13*, 165–177.
Williamson, D., McLennan, I. J., Bax, A., Gamcsik, M. P., & Glickson, J. D. (1990) *J. Biomol. Struct. Dyn. 8*, 375–398.
Xu, R. X., Antholine, W. E., & Petering, D. H. (1992a) *J. Biol. Chem. 267*, 944–949.
Xu, R. X., Antholine, W. E., & Petering, D. H. (1992b) *J. Biol. Chem. 267*, 950–955.